Design-based stereological study of the guinea-pig (Cavia porcellus) cerebellum

Design-based stereological study of the guinea-pig (*Cavia porcellus*) cerebellum

Running title: Guinea pig cerebellum stereology

Margherita De Silva[1], Javad Sadeghinezhad[2*], Jens Randel Nyengaard[3], Mahdi Aghabalazadeh Asl[2], Ava Saeidi[2], Nadia De Sordi[1], Roberto Chiocchetti[1], Annamaria Grandis[1]

[1]Department of Veterinary Medical Sciences (UNI EN ISO 9001:2008), University of Bologna, 40064, Ozzano dell'Emilia, Bologna, Italy

[2]Department of Basic Sciences, Faculty of Veterinary Medicine, University of Tehran, Tehran, Iran

[3]Core Centre for Molecular Morphology, Section for Stereology and Microscopy, Centre for Stochastic Geometry and Advanced Bioimaging, Aarhus University, Aarhus, Denmark

*Corresponding author: Javad Sadeghinezhad

Email: sadeghinezhad@ut.ac.ir

Abstract

Guinea pigs have proved useful as experimental animal models in studying cerebellar anatomical and structural alterations in human neurological disease; however, they are also currently acquiring increasing veterinary interest as companion animals. The morphometric features of the normal cerebellum in guinea pigs have not been previously investigated using stereology. The objective of the present work was to establish normal volumetric and quantitative stereological parameters for cerebellar tissues in guinea pigs, by means of unbiased design-based stereology. Cerebellar total volume, grey and white matter volume fractions, molecular and granular layers volume fractions, cerebellar surface area, Purkinje cellular and nuclear volumes, and the Purkinje cell total count were stereologically estimated. For this purpose, cerebellar hemispheres from six adult male guinea pigs were employed. Isotropic, uniform random sections were obtained by applying the orientator method, and subsequently processed for light microscopy. The cerebellar total volume, the white and grey matter volume fractions, and the molecular and granular layer volumes were estimated using the Cavalieri's principle and the point counting system. The cerebellar surface area was estimated through the use of test lines; Purkinje cellular and nuclear volumes were analysed using the nucleator technique, whereas the Purkinje cell total count was obtained by means of

the optical disector technique. The mean ± standard deviation (SD) total volume of a guinea-pig cerebellar hemisphere was 0.11±0.01 cm^3. The mean volumetric proportions occupied by the grey and white matters were, respectively, 78.0±2.6% and 22.0±2.6%, whereas their mean absolute volumes were found to be 0.21±0.02 cm^3 and 0.059±0.006 cm^3. The volumes of the molecular and granular layers were estimated at 112.4±20.6 mm^3 and 104.4±7.3 mm^3, whereas their mean thicknesses were calculated to be 0.184±0.020 mm and 0.17± 0.02 mm. The molecular and granular layers accounted for 40.7 ± 3.9 % and 37.4 ± 1.8 % of total cerebellar volume, respectively. The surface area of the cerebellum measured 611.4 ± 96.8 mm^2. Purkinje cells with a cellular volume of 3210.1 μm^3 and with a nuclear volume of 470.9 μm^3 had a higher incidence of occurrence. The mean total number of Purkinje cells for a cerebellar hemisphere was calculated to be 253,090 ± 34,754. The morphometric data emerging from the present study provide a set of reference data which might prove valuable as basic anatomical contribution for practical applications in veterinary neurology.

Keywords: Guinea pig, cerebellum, stereology, neuroanatomy, nervous system.

Introduction

The involvement of the cerebellum in motor coordination, balance and motor learning has been long and widely recognized (Brooks, 1984; Llinás and Welsh, 1993; Baillieux *et al.*, 2008; Lee *et al.*, 2015); however, a growing body of evidence involving neuroanatomical, neuroimaging and clinical studies indicates that it plays a significant role in non-motor behavioral-affective and cognitive functions, as well (Schmahmann and Caplan, 2006; Booth *et al.*, 2007; Molinari *et al.*, 2008; Cantalupo and Hopkins, 2010; Koziol *et al.*, 2011; De Smet *et al.*, 2013; Roostaei *et al.*, 2014).

Design-based stereological techniques allow to efficiently acquire accurate and precise quantitative estimates of three-dimensional morphometric features of whole organs from measurements made on two-dimensional sections, by making use of statistical sampling and stochastic geometry principles (Boyce *et al.*, 2010).

Most stereological investigations on the cerebellum involving laboratory animals have been carried out on mice (Woodruff-Pak, 2006; Woodruff-Pak *et al.*, 2010; Wittmann and McLennan, 2011; Kennard *et al.*, 2013; Song *et al.*, 2014), rats (Korbo *et al.*, 1993; Larsen *et al.*, 1993, 2000; Ragbetli *et al.*, 2007; Sonmez *et al.*, 2010) and rabbits (Akosman *et al.*, 2011; Selçuk and Tıpırdamaz, 2020), but also on domestic animals such as

84 cats (Sadeghinezhad *et al.*, 2020), pigs (Jelsing *et al.*, 2006) and chicks
85 (Tunç *et al.*, 2006). Apart from a stereological study performed on prenatal
86 and neonatal guinea-pig cerebella following experimentally-induced
87 intrauterine growth restriction (Mallard *et al.*, 2000), the morphometric
88 features of the normal cerebellum in adult animals of this species have not
89 been previously investigated using stereological techniques.

90 Guinea pigs (*Cavia porcellus*) have proved useful as experimental
91 animal models in studying cerebellar anatomical and structural alterations
92 in human neurological disease (Lev-Ram *et al.*, 1993; Furuoka *et al.*, 2011;
93 Čapo *et al.*, 2015; Bennet *et al.*, 2017; Cumberland *et al.*, 2017), partly due
94 to their high degree of neurological maturity at birth in relation to the short
95 gestation period (Altman and Das, 1967; Hargaden and Singer, 2012; Silva
96 *et al.*, 2016), which is important for clinical studies in human medicine.
97 Indeed, the brain of newborn guinea pigs is singularly mature, and
98 postnatal cerebellar neurogenesis is minimal in this precocial species
99 (Altman and Das, 1967). It was observed that, as early as 45 days through
100 gestation, cerebellar layers in guinea-pig fetuses were distinct and well
101 developed, with easily identifiable Purkinje cells, and with the white and
102 gray matters well differentiated both macro- and microscopically (Silva *et*
103 *al.*, 2016). Moreover, cellular proliferation events in the cerebellum, unlike
104 other rodents, are complete at birth in the guinea pig (Lossi *et al.*, 1997).

105 Recently, however, increasing interest has been addressed toward the
106 clinical features, pathological changes and therapeutic resolution of
107 neurological disorders of guinea pigs held as pet animals (Hollamby, 2009;
108 Hawkins and Bishop, 2012). Most incidences of naturally-occurring
109 cerebellar pathology reported in the literature for pet guinea pigs have an
110 infectious etiology. Reported aetiological agents are, for instance, the
111 lymphocitic choriomeningitis virus, leading to cerebellar hypoplasia with
112 acute destruction of cortex folia and necrosis of granule and Purkinje cells
113 (Monjan *et al.*, 1971; Hawkins and Bishop, 2012); *Toxoplasma gondii,*
114 inducing granulomatous meningoencephalitis, foci of necrosis, and chronic
115 cysts in the central nervous system (Brabb *et al.*, 2012; Gentz and
116 Carpenter, 2012); and *Bayilisascaris procionis* larvae, causing progressive
117 multifocal encephalomalacia and eosinophilic granulomatous inflammation
118 of the cerebellum, midbrain and brainstem (Van Andel *et al.*, 1995).
119 In light of the above-listed scientific evidence, the objective of the
120 present work was to establish normal volumetric and quantitative
121 stereological parameters for cerebellar tissues in adult guinea pigs, by
122 means of unbiased design-based stereology (Gundersen and Jensen, 1987;
123 West, 1993; Boyce *et al.*, 2010). Specifically, the present study was
124 designed to estimate cerebellar total volume, grey and white matter volume
125 fractions, molecular and granular layers volume fractions [by using the

126 Cavalieri 's principle (Gundersen and Jensen, 1987)], estimate the
127 cerebellar surface area (Schmitz and Hof, 2005), the total number of
128 Purkinje cells [by employing the optical disector method (Gundersen,
129 1977; Sterio, 1984)], and the mean Purkinje cellular and nuclear volumes
130 [through the use of the nucleator method (Gundersen *et al.*, 1988b)] in the
131 guinea pig.

132 The morphometric data emerging from the present study provide an
133 accurate set of reference data potentially valuable as basic anatomical
134 contribution to the field of veterinary neurology in order to help
135 implementing the development of the diagnosis and treatment of nervous
136 diseases in the guinea pig.

137

138 **Methods**

139 **Animals and tissue preparation**

140 Six adult male pet guinea pigs, weighing 569 ± 64.9 g, which
141 spontaneously died of diseases other than those affecting the nervous
142 system, were used for our research purposes following owners' permission.
143 The animals did not present a history of neurological disease nor displayed
144 pathological alterations of nervous tissues.

145 According to Directive 2010/63/EU of the European Parliament and
146 of the 22 September 2010 Council on the protection of animals used for

147 scientific purposes, the Italian legislation (D. Lgs. n. 26/2014) does not
148 require any approval by competent authorities or ethical committees, as this
149 research did not influence any therapeutic decisions.

150 Guinea-pig cerebella were excised from the neurocranium in their
151 entirety, each was divided into two halves, and then immersed in a 4%
152 phosphate-buffered formaldehyde solution to enable tissue fixation. One
153 hemisphere of each cerebellum was randomly chosen and weighed on a
154 digital laboratory scale. The cerebellar hemispheres were routinely
155 processed for light microscopic examination and subsequently embedded in
156 paraffin.

157 **Tissue sampling and stereology**

158 The orientator method (Mattfeldt *et al*., 1990; Nyengaard, 1999) was
159 applied to obtain isotropic, uniform, random sections. In essence, each
160 cerebellar hemisphere was embedded in a paraffin block, which was placed
161 at the center of a circle with 90 equidistant divisions along the perimeter. A
162 random number between 0 and 90 was looked up and the paraffin medium
163 was cut along a line parallel to the direction of the selected number. The
164 block was placed on its cut surface at the center of a second circle, with 96
165 nonequidistant divisions along its perimeter. The paraffin was cut along a
166 line parallel to the direction of a random number ranging from 0 to 96, and
167 the block was finally re-embedded in paraffin while placed on its cut

surface (Fig. 1). Consecutive 25 micrometer-thick sections were cut with a microtome at uniform constant intervals with a random start and until exhausting the organ. Every 25th section was collected using the principle of systematic uniform random sampling (Gundersen and Jensen, 1987), in order to acquire 12 to 15 sections per animal. Sections were then stained with Cresyl violet 0.1 % stain solution. A slide scanner (Optic lab H850, Plustek) was employed for capturing images from sections in order to enable the subsequent estimation of volumes and surface areas. A microscope (CX40, Olympus, Germany) equipped with an oil immersion objective (×100), connected to a microcator (MT12, Heidenhain, Traunreut, Germany) and a digital camera (MB-225) was utilized for the estimation of Purkinje cells total cellular and nuclear volumes. Geometrical probes, necessary for the stereological analysis of each structural feature represented in each section (West, 1993), were produced using a dedicated software (ImageJ; https://imagej.nih.gov).

Estimation of total and fractional volumes

The accurate estimation of cerebellar total volume was made possible by employing cerebellar weight and transforming it into a volume, and by applying the Cavalieri's estimator, taking therefore into account tissue shrinkage. Cerebellar shrinkage secondary to histological processing allows to obtain unbiased stereological estimations insensitive to

189 processing-dependent tissue deformations (Dorph-Petersen *et al*., 2001).

190 The estimation of total volume starting from the weight of the

191 cerebellum, was performed using the following formula:

192 $V\ (cerebellum) = W\ (cerebellum) / \rho$,

193 where ρ refers to the weight-to-volume ratio of cerebellar tissue.

194 The estimation of the total volume of the cerebellum through use of the

195 Cavalieri principle was conducted by using the test point system (Fig. 2)

196 and following the equation below (Howard and Reed, 1998):

197 $V = \Sigma P \cdot SSF \cdot T \cdot (a/p)$

198 where ΣP is the total number of points hitting the structure; SSF (1/25)

199 represents the section sampling fraction; T (25 μm) is the section thickness

200 and a/p (465,267 μm^2) refers to the area per point.

201 The fractional volume (V_v) of cerebellar structures including white

202 matter, grey matter, molecular and granular layers, was estimated using the

203 following formula (Gundersen *et al.*, 1988a):

204 $V_v\ (structure) = \sum P\ (structure) / \sum P\ (cerebellum)$

205 where $\sum P$ (structure) is the number of points hitting the white matter, gray

206 matter, molecular and granular layers, and $\sum P$ (cerebellum) is the number

207 of points hitting the cerebellum.

208 Lastly, in order to estimate the volume accounted for by each

209 structure, each volume fraction was multiplied by the total volume of the

210 cerebellum.

211 **Estimation of surface area**

212 The surface density (S_v) of the cerebellum was estimated by using
213 test lines (Fig. 2b), and by employing the following formula (Howard and
214 Reed, 1998):

215 $S_v = 2 \cdot \sum l / (\sum P \cdot l/p)$

216 Where $\sum l$ represents the total number of intersections between the outer
217 surface of the cerebellum and the test lines, $\sum P$ refers to the points hitting
218 the molecular layer, l/p (658 μm) was the length of each test line associated
219 to each point of the test grid.

220 Consequently, for estimating the surface area, surface density was multiped
221 by the volume of the molecular layer.

222 In addition, the thickness (T) of the molecular and granular layers was
223 calculated using the following formula (Andersen *et al.*, 2012):

224 T (layer) = V (layer) ⁄ S (layer)

225 where V is the volume and S is the surface area of each layer.

226 **Estimation of Purkinje cell total count**

227 The optical disector method was employed for the estimation of the
228 Purkinje cell total number, and a motorized stage designed by Department
229 of Anatomy, Faculty of Veterinary Medicine, of the University of Tehran,
230 Tehran, Iran, was employed for the purpose. The microscopic fields were

231 selected by moving the microscope stage in the x and y directions for a
232 constant distance spanning the entire section thickness. The unbiased
233 counting frame principle was applied for counting the cells. The Purkinje
234 cells whose nucleolus was located inside the counting frame or crossed the
235 accepted lines were sampled, and those whose nucleolus came into focus
236 within disector height were counted (Fig. 3).
237 The numerical density of Purkinje cells was calculated using the following
238 formula (Kristiansen and Nyengaard, 2012):
239 N_v (Purkinje cells) = $[\Sigma Q^- / (a/f \times \Sigma P \times h)] \times t/BA$

240 where ΣQ^- represents the total count of Purkinje cells, *a/f* (9895 μm^2) is the
241 area per frame, ΣP is the total number of frames, *h* (10 μm) is the disector
242 height, *t* is the sections mean thickness (18.5 μm), measured for each
243 microscopic field, and BA (25 μm) is the block advance.

244 Finally, for the estimation of the total number of Purkinje cells, the
245 numerical density was multiplied by the total volume of the cerebellum,
246 estimated using the Cavalieri's principle.

247 **Estimation of mean Purkinje cellular and nuclear volumes**

248 To estimate the volumes of Purkinje cells and Purkinje cell nuclei,
249 the nucleator technique was utilized (Gundersen *et al.*, 1988b). The volume
250 of the sampled cells was measured by using the unbiased counting frame,

251 and following the formula (Gundersen *et al.*, 1988b):

252 $V_n = 4\pi/3 \cdot l_n^3$

253 Where l_n refers to the intercept length from the nucleolus to the border of
254 the cytoplasm (for cellular volume), or to the border of the nucleus (for
255 nuclear volume) of Purkinje cells.

256 **Estimation of the coefficient of error (CE)**

257 The precision of the volume estimates, expressed in terms of CE, is
258 related to the variability associated with systematic uniform random
259 sampling (SURS) sampling and point counting of the estimator. The CE for
260 the estimate of the volume (Gundersen and Jensen, 1987), surface area
261 (Kroustrup and Gundersen, 1983) and Purkinje cell count (Braendgaard *et*
262 *al.*, 1990) was calculated.

263

264 **Statistical analysis**

265 All data are expressed as mean ± standard deviation (SD). As for
266 right-skewed distributions, a logarithmic scale was used for individual
267 estimates of Purkinje cellular and nuclear volumes (Weber *et al.*, 1997).

268

269 **Results**

270 All cerebella evaluated appeared normal both macroscopically and
271 on histological examination, with all the microscopical structures being

distinctly identifiable and without any evidence of pathological processes.

The mean (±SD) weight of a guinea-pig cerebellar hemisphere was 0.285 ± 0.028 g. The mean volume of a guinea pig cerebellar hemisphere, calculated by dividing the cerebellar weight by its specific gravity, was 0.274 ± 0.027 cm^3, while the value obtained by employing the Cavalieri's estimator, was 0.110 ± 0.015 cm^3. A 61.34 ± 5.39% total cerebellar volume shrinkage, secondary to the process of paraffin embedding, was estimated. The relative volume fractions of the grey and white matters, expressed as a percentage of total cerebellar volume, were found to be 78.06 ± 2.66% and 21.92 ± 2.67%, respectively. Their absolute volumes, on the other hand, were calculated to be 0.21 ± 0.02 cm^3 for the grey matter, and 0.060 ± 0.006 cm^3 for the white matter. The separate and mean values for the above-mentioned parameters, are outlined in Table 1.

The surface area of the cerebellum measured 611.4 ± 96.8 mm^2. The volume of the molecular layer was estimated to be 112.41 ± 20.56 mm^3 while that of the granular layer 104.38 ± 7.31 mm^3; the molecular and granular layers accounted for 40.67 ± 3.87 % and 37.38 ± 1.77 % of total cerebellar volume, respectively. The mean thickness of the molecular and granular layers was 0.184±0.020 mm and 0.169 ± 0.017 mm, respectively. In Table 2 are shown the mean and individual data calculated for the above-mentioned criteria in the six guinea pigs.

293 The frequency distribution of the Purkinje cellular and nuclear
294 volumes is plotted in Fig. 4. The Purkinje cell volumes were found to be
295 ranging from 987 to 8246.8 μm^3, of which cells with a volume of 3210.1
296 μm^3 had a higher (13.71%) incidence of occurrence. The estimated volume
297 of Purkinje nuclei was found to be ranging between <117 and 1623.4 μm^3,
298 and nuclei with a volume of 470.9 μm^3 were the most frequently occurring
299 ones (13.54%).
300 The mean total number of Purkinje cells for a cerebellar hemisphere
301 was calculated to be 253,090 ± 34,754 (Table 3).
302 The mean coefficient of error (CE) and coefficient of variation (CV),
303 along with their ratio (CE^2/CV^2), calculated for total cerebellar volume,
304 grey and white matter volume fractions, granular and molecular layers
305 volume fractions, cerebellar surface area, and total number of Purkinje cells
306 are shown in Table 4.
307
308 **Discussion**
309 The mean total volume of a guinea-pig cerebellar hemisphere
310 estimated in the present study is consistent with that calculated in a
311 previous work, which investigated the brain morphology of domestic
312 guinea pigs through quantitative cytoarchitectonic measurements (Kruska,
313 2014). Cerebellar total volume has been previously assessed by

314 stereological techniques in other species such as humans, which exhibited a
315 difference between sexes, with male cerebella measuring 120.5 ± 11.1 cm^3
316 in volume, while females 105.9 ± 11.2 cm^3 (Taman *et al.*, 2020). Cerebellar
317 volume has also been stereologically estimated in rabbits (Karabekir *et al.*,
318 2014) and rats (Noorafshan *et al*., 2018), presenting volumes of 0.69 ± 0.03
319 cm^3, and 0.080 ± 0.004 cm^3 for each cerebellar hemisphere, respectively,
320 but also in cats (Sadeghinezhad *et al.*, 2020), presenting a mean cerebellar
321 hemisphere volume of 2.06 ± 0.29 cm^3. When comparing total cerebellar
322 volume (in cm^3) in relation to body weight (in kg) in each species, it
323 appears that the guinea pigs of the present study have a cerebellar volume
324 to body weight ratio of 0.9, which is consistent with the 0.8 calculated for
325 the rat (Noorafshan *et al.*, 2018), but greater than the 0.4 estimated for the
326 rabbit (Karabekir *et al.*, 2014), and less than an approximate 1.7 for an
327 adult individual of average weight (Taman *et al.*, 2020) and than the
328 approximate 1.1 calculated for a medium-sized cat (Sadeghinezhad *et al.*,
329 2020).

330 The cerebellar weight to body weight ratio was 0.1 in the guinea pig
331 study population, which is in line with an approximate 0.13 calculated for a
332 medium-sized cat (Sadeghinezhad *et al.*, 2020). Cerebellar volumetric
333 modifications have been correlated with physiological factors such as age,
334 gender (Raz *et al.*, 1998), cognitive capability, but also with several

335 pathological neurological conditions such as Alzheimer's disease,
336 schizophrenia and epilepsy in humans (Bottmer *et al.*, 2005; Sato *et al.*,
337 2007; Bas *et al.*, 2009; Andersen *et al.*, 2012). A study carried out on rats
338 has also identified a correlation between maternal diabetes and a reduction
339 of total cerebellar volume and thickness of all layers in the offspring (Hami
340 *et al.*, 2016). Volumetric prediction of the cerebellum can therefore find a
341 valuable use in further research on veterinary neurological disease affecting
342 cognition.

343 The cerebellar gray and white matter volumes have also been
344 sterologically estimated in other species. The total gray matter volume of
345 human cerebella has been calculated to be 88.5 cm^3, while that of the white
346 matter 22.5 cm^3 (Andersen *et al.*, 2012). Cerebellar grey and white matter
347 volumes were estimated to be 1.46 ± 0.24 cm^3 and 0.60 ± 0.06 cm^3,
348 respectively, for the cat (Sadeghinezhad *et al.*, 2020). When compared to
349 the guinea pig and cat, the proportionally more voluminous grey matter in
350 humans can be likely ascribed to their increased development of motor
351 control, coordination, as well as cognitive functions. Moreover, it was
352 noted that, in the early domesticated mammals such as the guinea pig, a
353 decrease in total brain size, which is proportional to the level of
354 encephalization of the species, along with a decrease in total cortex and
355 areas responsible for processing sensory information and motor control,

356 such as the grey matter, occurred as a consequence of the domestication
357 process, with, however, the cognitive functions not being affected by this
358 change (Kruska, 2005; Kaiser *et al.*, 2015; Welniak-Kaminska *et al.*, 2019).
359 The volumes of the grey and white matter calculated in the present study
360 are markedly greater than those reported by Mallard *et al.* (2000) for
361 neonatal guinea pigs, which is likely due to the large age and body weight
362 discrepancy. The influence of the physiological process of aging on
363 volumetric changes in the cerebellar gray and especially the white matter
364 has been assessed in several studies (Jernigan *et al.*, 2001; Walhovd *et al.*,
365 2005).
366 Several human neurological diseases affecting cognition have also been
367 observed to cause volume losses of the cerebellar gray and white matters
368 (Fennema-Notestine *et al.*, 2004; Anderson *et al.*, 2009), as evidence of the
369 role that the cerebellum plays in cognition.
370 The mean volumes of the molecular and granular layers in the guinea
371 pig cerebellum estimated in the present work are significantly greater than
372 the corresponding values reported by Mallard *et al.* (2000) for neonatal
373 guinea pigs, and, comparing the two studies, the volumes of the two layers
374 are apparently not proportionally related to body weight. The mean
375 corresponding volumes referring to humans are 54.4 cm^3 for the molecular
376 layer, and 37.9 cm^3 for the granular layer (Andersen, 2004). The mean

volume of the molecular and granular layers of the cerebellum of normal rats was reported to be 0.035 cm^3 and 0.024 cm^3, respectively (Dortaj *et al*., 2018). In cats' cerebella, the mean molecular layer volume had been reported to be 0.89 ± 0.16 cm^3, while that of the granular layer 0.56 ± 0.10 cm^3 (Sadeghinezhad *et al.*, 2020). The relative proportions of the molecular and granular layers of the cerebellum in the different species seem to be conserved, thanks to the similar cerebellar microscopical anatomy. As a matter of fact, the histological examination of the guinea pig cerebella permitted the clear identification of the molecular, Purkinje and granular layers with their characteristic cellular populations. The conserved volumetric trend seems to be therefore related to function.

A stereological study carried out on intrauterine growth-restricted guinea pigs secondary to placental insufficiency in the second half period of pregnancy, has been seen to cause a reduction in the volume of the molecular and granular layers, as well as in that of the white matter in prenatal guinea-pig cerebella, therefore causing cognitive, motor and behavioral deficits in the post-natal life (Mallard *et al.*, 2000).

When analyzing the distribution of the thickness of the molecular and granular layers in the different subjects comprising our study population, it appears that the measurements are quite consistent and

397 regular, in contrast with what Sultan and Braitenberg (1993) had reported
398 for smaller mammalian species. Andersen (2004) calculated a mean
399 thickness of the molecular layer of 590.00 ± 0.08 μm and 410.00 ± 0.15 μm
400 for the granular layer in human cerebella. Sadeghinezhad *et al.* (2020), on
401 the other hand, calculated 133.5 ± 10.1 μm for the molecular layer and 84.7
402 ± 17.3 μm for the granular layer in cats' cerebella. Consistently with human
403 and cats' cerebella, the molecular layer appears thicker than the granular,
404 although not in a statistically significant manner; however, it seems that the
405 thickness in guinea pigs is more uniformly-distributed between the two
406 layers when compared to cats and humans' data. This can be explained by
407 different physiological factors such as age. Indeed, a study carried out on
408 cats' cerebella showed that aging causes an increase in granular layer
409 thickness at the expense of that of the molecular layer (Zhang *et al*., 2006).

410 With regard to the measurement of the cerebellar surface area, the
411 ratio of cerebellar surface area to cerebellar weight in the different animals
412 comprising the study population remains fairly constant, supporting the
413 proportionality between cerebellar area and cerebellar weight hypothesized
414 by Sultan and Braitenberg for larger mammals (1993), which is probably
415 due, unlike other smaller mammalian species, to the equally constant
416 distribution of grey matter thickness values in our guinea pig population.
417 Further studies on larger population samples are needed to confirm this

418 finding. The average surface area of the human cerebellum has been
419 previously estimated by different authors to be 550 cm^2 (Henery and
420 Mayhew, 1989), 1027 cm^2 (Andersen *et al.*, 2012) and 1160 cm^2 (Andersen
421 *et al.*, 1992). The human cerebellum, during evolution, underwent a
422 significant expansion of its surface area both in absolute terms as well as in
423 relation to the neocortex; this growth played a critical role in human
424 cognitive development in comparison with other animals, given the role of
425 the cerebellum in cognition (Barton and Venditti, 2014). In the animal
426 kingdom, therefore, it is likely that the cerebellar surface area of highly
427 encephalized species such as higher primates might show a greater
428 development in comparison with mammals of a similar size. On the other
429 hand, a mild but significant reduction in the total cerebellar area has been
430 described in humans with advancing age, showing varying decline trends in
431 the different vermian lobules (Raz *et al.*, 1998). A study carried out on
432 experimentally vitamin C-deprived guinea pig fetuses has revealed a
433 significant reduction in cerebellar surface area due to the obliteration of
434 fissures and the fusion of opposing folia, resulting in a macroscopically-
435 visible cerebellar dysplasia in terms of flattening of its surface, analogously
436 to that observed in Lyssencephaly Type 2 (Čapo *et al.*, 2015). The
437 mentioned study is of clinical relevance in pet guinea pigs due to their
438 natural incapability of endogenous vitamin C synthesis (Nishikimi *et al.*,

439 1992), analogously to humans, resulting in the necessity of its dietary
440 supplementation, with the risk of developing vascular as well as
441 neurological disease in case of deprivation.

442 Purkinje cells with a perikaryon volume of 3210.1 μm^3 and with a
443 nuclear volume of 470.9 μm^3 were found to have the highest frequency of
444 occurrence in the guinea pig cerebellum. Mean Purkinje cellular perikaryon
445 volumes had been estimated to be 12400 μm^3 in humans (Korbo and
446 Andersen, 1995), 4900 μm^3 (Korbo and Andersen, 1995) and 5600 μm^3
447 (Sørensen *et al.*, 2000) in rats, 17600 μm^3 in adult minipigs (Jelsing *et al.*,
448 2006), 2207 μm^3 in rabbits (Akosman *et al.*, 2011), and 6994 μm^3 in cats
449 (Sadeghinezhad *et al.*, 2020). If considering a mean weight for an adult
450 individual of each species, and calculating a ratio of Purkinje volume to
451 body weight, these findings suggest a non-allometric correlation. Indeed,
452 the mini-pig (Jelsing *et al.*, 2006) has a Purkinje volume to body weight
453 ratio that is six times greater than that of humans (Korbo and Andersen,
454 1995), whereas rodents such as the rat (Sørensen *et al.*, 2000) and the
455 guinea pig have, respectively, ratios that are 40 and 180 times
456 proportionally greater than that of humans. The variability encountered
457 might be explained by the different degrees of tissue shrinkage (Andersen
458 *et al*., 1992), by the immersion time of the tissue in the fixative (Jelsing *et*
459 *al*., 2006), by the degree of postnatal development of Purkinje perikaryon

460 volume (Jelsing *et al*., 2006), or by different degrees of significance of
461 Purkinje cell roles in motor, sensory and cognitive functions among the
462 different species.

463 The mean total number of Purkinje cells calculated in the present
464 work is consistent with the value reported for the whole cerebellum in a
465 previous work carried out on neonatal guinea pigs, that is in the order of
466 500,000 (Mallard *et al.*, 2000). It has been demonstrated that the brain of
467 newborn guinea pigs, species characterized by its precocity, presents a high
468 degree of neurological maturity, and that postnatal cerebellar neurogenesis
469 is minimal (Altman and Das, 1967). As a matter of fact, all cerebellar
470 layers, including Purkinje cells, as well as white and gray matters, are well
471 developed and differentiated as early as 45 days post conception (Silva *et*
472 *al.*, 2016), and that all cerebellar cell proliferation events are entirely
473 complete at birth in this species, unlike other similar rodents (Lossi *et al.*,
474 1997). In the adult mini-pig cerebellum, on the other hand, the total number
475 of Purkinje cells was in the order of 2.8 million (Jelsing *et al*., 2006). The
476 numerosity of the Purkinje cell count in the above-mentioned study was,
477 indeed, partially explained by a significant postnatal development in total
478 Purkinje cell number and perikaryon volume, as it had also been
479 demonstrated in rats (Altman and Bayer, 1978), humans (Miyata *et al*.,
480 1999), and cats (Vastagh *et al*., 2005). The total number of Purkinje cells in

481 the whole adult rat cerebellum was estimated at around 320,000 cells
482 (Sonmez *et al.*, 2010), which is markedly less than the value obtained for
483 the guinea pig, and that could be explained by the complex heterogeneity of
484 guinea pigs' Purkinje cells. It has been noted that Purkinje cells in the
485 guinea pig cerebellum show a complex expression pattern of zebrin II, an
486 immunohistochemical marker of cerebellar compartmental heterogeneity,
487 showing three levels of zebrin II expression (Larouche *et al.*, 2003), as
488 opposed to rats, where zebrin II expression only distinguishes two classes
489 of Purkinje cells (Brochu *et al.*, 1990).

490 The hypothesis that less voluminous brains tend to have a higher cellular
491 density than larger brains (Mwamengele *et al.*, 1993) does not seem to
492 always be applicable, as is the case with the higher count of Purkinje cells
493 in the guinea pigs comprising the present study when compared with the
494 values reported for the rat (Sonmez *et al.*, 2010). Reports of acquired
495 cerebellar degenerative disease in pet guinea pigs, mostly secondary to an
496 infectious etiology, have been described in the literature, with ataxia and
497 loss of voluntary motor control being common clinical signs, and
498 meningoencephalitis and cerebellar cortical hypoplasia with necrosis of
499 granule and Purkinje cells the principal histopathological findings (Monjan
500 *et al.*, 1971; Van Andel *et al.*, 1995; Brabb *et al.*, 2012; Gentz and
501 Carpenter, 2012; Hawkins and Bishop, 2012).

502 In conclusion, the present study represents the first detailed
503 description of the morphometrical features of the guinea pig cerebellum
504 using design-based stereological techniques. The reference morphometrical
505 data provided for cerebellar structures might find a use as basic anatomical
506 contribution to a greater understanding of neurological diseases when
507 examining cerebellar pathology with relation to function in this exotic pet
508 species of increasing veterinary interest. In addition, the present study
509 might prove useful by providing a comparison with available data in
510 humans and other mammals for future research investigating the basis of
511 motor, cognitive and behavioral diseases in the different species.

512

513

514

515

516 **Conflict of interests**

517 The authors have no conflict of interests to declare.

518 **Author contributions**

519 M.D.S.: acquisition of data, data analysis/interpretation, drafting of the

manuscript; J.S.: concept/design, acquisition of data, data analysis/interpretation, critical revision and approval of the manuscript; J.R.N.: data analysis/interpretation, critical revision of the manuscript and approval of the article; M.A.A.: data analysis/interpretation; A.S.: data analysis/interpretation; N.D.S.: acquisition of data; R.C.: concept/design; critical revision of the manuscript and approval of the article; A.G.: acquisition of data, critical revision of the manuscript and approval of the article.

References

Akosman, M.S., Gocmen-Mas, N. and Karabekir, H.S. (2011) Estimation of Purkinje cell quantification and volumetry in the cerebellum using a stereological technique. *Folia Morphologica (Warsz),* **70**, 240-244.

Altman, J. and Bayer, S.A. (1978) Prenatal development of the cerebellar

system in the rat. I. Cytogenesis and histogenesis of the deep nuclei and the cortex of the cerebellum. *Journal of Comparative Neurology*, **179**, 23-48. doi: 10.1002/cne.901790104.

Altman J. and Das, G. (1967) Postnatal Neurogenesis in the Guinea pig. *Nature*, **214,** 1098–1101. https://doi.org/10.1038/2141098a0

Andersen, B. B. (2004) Reduction of Purkinje cell volume in cerebellum of alcoholics. *Brain Research*, **1007**, 10-18. doi: 10.1016/j.brainres.2004.01.058

Andersen, B. B., Korbo, L. and Pakkenberg, B. (1992) A quantitative study of the human cerebellum with unbiased stereological techniques. *Journal of Comparative Neurology*, **326**, 549-460. doi: 10.1002/cne.903260405

553 Andersen, K., Andersen, B.B. and Pakkenberg, B. (2012) Stereological
554 quantification of the cerebellum in patients with Alzheimer's disease.
555 *Neurobiology of Aging*, **33**, 197.e11-20.

556 Anderson, V. M., Fisniku, L. K., Altmann, D. R., Thompson, A. J and
557 Miller, D. H. (2009) MRI measures show significant cerebellar gray matter
558 volume loss in multiple sclerosis and are associated with cerebellar
559 dysfunction. *Multiple Sclerosis Journal*, **15**, 811-817. doi:
560 10.1177/1352458508101934

561 Baillieux, H., De Smet, H.J., Paquier, P.F., De Deyn, P.P. and Marien, P.
562 (2008) Cerebellar Neurocognition: Insights into the bottom of the brain.
563 *Clinical Neurology and Neurosurgery*, **110**, 763-773.

564 Barton, R. A. and Venditti, C. (2014) Rapid evolution of the cerebellum
565 in humans and other great apes. *Current Biology*, **24**, 2440-1444. doi:
566 10.1016/j.cub.2014.08.056

567 Bas, O., Acer, N., Mas, N., Karabekir, H. S., Kusbeci, O. Y. and Sahin,
568 B. (2009) Stereological evaluation of the volume and volume fraction of
569 intracranial structures in magnetic resonance images of patients with
570 Alzheimer's disease. *Annals of Anatomy*, **191**, 186-195. doi:
571 10.1016/j.aanat.2008.12.003

572 Bennett, G.A., Palliser, H.K., Shaw, J.C., Palazzi, K.L., Walker, D.W. and

573 Hirst, J.J. (2017) Maternal stress in pregnancy affects myelination and
574 neurosteroid regulatory pathways in the guinea pig cerebellum. *Stress*, **20**,
575 580-588.

576 Booth, J.R., Wood, L., Lu, D., Houk, J.C. and Bitan, T. (2007) The role
577 of the basal ganglia and cerebellum in language processing. *Brain*
578 *Research*, **1133**, 136-144.

579 Bottmer, C., Bachmann, S., Pantel, J., Essig, M., Amann, M., Schad,
580 L.R. and Schröder, J. (2005) Reduced cerebellar volume and neurological
581 soft signs in first-episode schizophrenia. *Psychiatry Research*, **140**, 239–
582 250.

583 Boyce, R.W., Dorph-Petersen, K.A., Lyck, L. and Gundersen, H.J.G.
584 (2010) Design-based stereology: introduction to basic concepts and
585 practical approaches for estimation of cell number. *Toxicologic Pathology*,
586 **38**, 1011-1025.

587 Brabb, T., Newsome, D., Burich, A. and Hanes, M. (2012) Guinea pigs:
588 infectious diseases. In: Suckow, M.A., Stevens, K.A. and Wilson, R.P.
589 (Eds) The laboratory rabbit, guinea pig, hamster, and other rodents. San
590 Diego, Elsevier, pp. 638-683.

591 Braendgaard, H., Evans, S.M., Howard, C.V. and Gundersen, H.J. (1990)
592 The total number of neurons in the human neocortex unbiasedly estimated
593 using optical disectors. *Journal of Microscopy*, **157**, 285-304.

594 doi: 10.1111/j.1365-2818.1990.tb02967.x.

595 Brooks, V.B. (1984) Cerebellar functions in motor control. *Human*
596 *Neurobiology*, **2**, 251-260.

597 Brochu, G., Maler, L. and Hawkes, R. (1990) Zebrin II: A polypeptide
598 antigen expressed selectively by purkinje cells reveals compartments in rat
599 and fish cerebellum. *Journal of Comparative Neurology*, **291**, 538-552.
600 doi: 10.1002/cne.902910405

601 Cantalupo, C. and Hopkins, W. (2010) The cerebellum and its
602 contribution to complex tasks in higher primates: A comparative
603 perspective. *Cortex*, **46**, 821-830.

604 Čapo, I., Hinić, N., Lalošević, D., Vučković, N., Stilinović, N.,
605 Marković, J. and Sekulić, S. (2015) Vitamin C depletion in prenatal guinea
606 pigs as a model of lissencephaly type II. *Veterinary Pathology*, **52**, 1263-
607 1271.

608 Cavalieri, B. (1635) Geometria Indivisibilibus Continuorum. Nova
609 Quadam Ratione Promota. Bononiae. Typis Clementis Fernoij. Reprinted
610 as Geometria degli Indivisibili. Unione Tipografico-Editrice Torinese,
611 Torino, Italy, 1966.

612 Cumberland, A.L., Palliser, H.K., Walker, D.W. and Hirst, J.J. (2017)
613 Cerebellar changes in guinea pig offspring following suppression of
614 neurosteroid synthesis during late gestation. *The Cerebellum*, **16**, 306-313.

De Smet, H.J., Paquier, P., Verhoeven, J. and Marien, P. (2013) The cerebellum: Its role in language and related cognitive and affective functions. *Brain and Language*, **127**, 334-342.

Dorph-Petersen, K.A., Nyengaard, J.R. and Gundersen, H.J. (2001) Tissue shrinkage and unbiased stereological estimation of particle number and size. *Journal of Microscopy*, **204**, 232-246. doi: 10.1046/j.1365-2818.2001.00958.x..

Dortaj, H., Yadegari, M., Hosseini Sharif Abad, M., Abbasi Sarcheshmeh, A. and Anvari, M. (2018) Stereological Method for Assessing the Effect of Vitamin C Administration on the Reduction of Acrylamide-induced Neurotoxicity. *Basic and Clinical Neuroscience*, **9**, 27-34. doi: 10.29252/nirp.bcn.9.1.27

Fennema-Notestine, C., Archibald, S. L., Jacobson, M. W., Corey-Bloom, J., Paulsen, J. S., Peavy, G. M. *et al*. (2004) In vivo evidence of cerebellar atrophy and cerebral white matter loss in Huntington disease. *Neurology*, **63**, 989-995. doi: 10.1212/01.wnl.0000138434.68093.67

Furuoka, H., Horiuchi, M., Yamakawa, Y. and Sata, T. (2011) Predominant involvement of the cerebellum in guinea pigs infected with bovine spongiform encephalopathy (BSE). *Journal of Comparative Pathology*, **144**, 269-276.

635 Gentz, E. and Carpenter, J.W. (2012) Neurologic and musculoskeletal
636 disease. In: Hillyer, E.V. and Quesenberry, K.E. (Eds) Ferrets, rabbits and
637 rodents: clinical medicine and surgery. Philadelphia, WB Saunders, pp.
638 220-226.

639 Gundersen, H.J.G. (1977) Notes on the estimation of the numerical
640 density of arbitrary profiles: the edge effect. *Journal of Microscopy*, **111**,
641 219-223.

642 Gundersen, H.J.G. and Jensen, E.B. (1987) The efficiency of systematic
643 sampling in stereology and its prediction. *Journal of Microscopy*, **147**, 229-
644 263.

645 Gundersen, H.J., Bendtsen, T.F., Korbo, L., Marcussen, N., Mallei, A.,
646 Nielsen, K. *et al*. (1988a) Some new, simple and efficient stereological
647 methods and their use in pathological research and diagnosis. *Acta*
648 *Pathologica Microbiologica et Immunologica Scandinavica*, **96**, 379 –394.

649 Gundersen, H.J., Bagger, P., Bendtsen, T.F., Evans, S.M., Korbo, L.,
650 Marcussen, N. *et al*. (1988b) The new stereological tools: Disector,
651 fractionator, nucleator and point sampled intercepts and their use in
652 pathological research and diagnosis. *Acta Pathologica Microbiologica et*
653 *Immunologica Scandinavica*, **96**, 857–881.

654 Hami, J., Vafaei-Nezhad, S., Ghaemi, K., Sadeghi, A., Ivar, G., Shojae, F.
655 and Hosseini, M. (2016) Stereological study of the effects of maternal

656 diabetes on cerebellar cortex development in rat. *Metabolic Brain Disease*,
657 **31**, 643-652. doi: 10.1007/s11011-016-9802-5
658 Hargaden, M. and Singer, L. (2012) Anatomy, Physiology, and Behavior.
659 In: Suckow, M.A., Stevens, K.A. and Wilson, R.P. (eds) The laboratory
660 rabbit, guinea pig, hamster, and other rodents. San Diego, Elsevier, pp. 575-
661 602.
662 Hawkins, M.G. and Bishop, C.R. (2012) Disease problems of guinea
663 pigs. In: Queesenberry, K.E. and Carpenter, J.W. (Eds) Ferrets, rabbits and
664 rodents: clinical medicine and surgery. Philadelphia, Elsevier Saunders, p.
665 307.
666 Hollamby, S. (2009) Rodents: neurological and musculoskeletal
667 disorders. In: Keeble, E. and Meredith, A. (Eds) BSAVA manual of rodents
668 and ferrets. Gloucester, BSAVA, pp. 161-168.
669 Howard, C.V. and Reed, M.G. (1998) Unbiased stereology. Three-
670 dimensional measurement in microscopy. Bios Scientific Publishers,
671 Oxford, pp. 107–123.
672 Henery, C. C. and Mayhew, T. M. (1989) The cerebrum and cerebellum
673 of the fixed human brain: efficient and unbiased estimates of volumes and
674 cortical surface areas. *Journal of Anatomy*, **167**, 167-180.
675 Jelsing, J., Gundersen, H.J., Nielsen, R., Hemmingsen, R. and
676 Pakkenberg, B. (2006) The postnatal development of cerebellar Purkinje

677 cells in the Göttingen minipig estimated with a new stereological sampling
678 technique--the vertical bar fractionator. *Journal of Anatomy*, **209**, 321-331.
679 doi: 10.1111/j.1469-7580.2006.00611.x
680 Jernigan, T. L., Archibald, S. L., Fennema-Notestine, C., Gamst, A. C.,
681 Stout, J. C., Bonner, J and Hesselink, J. R. (2001) Effects of age on tissues
682 and regions of the cerebrum and cerebellum. *Neurobiology of Aging*, **22**,
683 581-594. doi: 10.1016/s0197-4580(01)00217-2

684

685 Kaiser, S., Hennessy, M.B. and Sachser, N. (2015) Domestication affects
686 the structure, development and stability of biobehavioural profiles.
687 *Frontiers in Zoology*, **12**, S19. doi: 10.1186/1742-9994-12-S1-S19.
688 Karabekir, H.S., Akosman, M.S., Gocmen-Mas, N., Aksu, F., Edizer, M.,
689 Lenger, O.F. and Turkmenoglu, I. (2014) The volume of experimental
690 design cerebellum: stereological microanatomic study. *Journal of*
691 *Craniofacial Surgery*, **25**, 1492-1494. doi:
692 10.1097/SCS.0000000000000845.
693 Kennard, J.A., Brown, K.L. and Woodruff-Pak, D.S. (2013) Aging in the
694 cerebellum and hippocampus and associated behaviors over the adult life
695 span of CB6F1 mice. *Neuroscience*, **247**, 335-350.
696 Korbo, L. and Andersen, B. B. (1995) The distributions of Purkinje cell
697 perikaryon and nuclear volume in human and rat cerebellum with the

698 nucleator method. *Neuroscience*, **69**, 151-158. doi: 10.1016/0306-
699 4522(95)00223-6

700 Korbo, L., Andersen, B.B., Ladefoged, O. and Møller, A. (1993) Total
701 numbers of various cell types in rat cerebellar cortex estimated using an
702 unbiased stereological method. *Brain Research*, **609**, 262-268.

703 Koziol, L.F., Budding, D.E. and Chidekel, D. (2011) From movement to
704 thought: executive function, embodied cognition, and the cerebellum. *The*
705 *Cerebellum*, **11**, 505-525.

706 Kristiansen, S.L.B. and Nyengaard, J.R. (2012) Digital stereology in
707 neuropathology. *Acta Pathologica Microbiologica et Immunologica*
708 *Scandinavica*, **120**, 327-340.

709 Kroustrup, J.P. and Gundersen, H.J.G. (1983) Sampling problems in an
710 heterogeneous organ: Quantitation of relative and total volume of
711 pancreatic-islets by light-microscopy. *Journal of Microscopy*, **132**, 43–55.

712 Kruska, D.C.T. (2005) On the evolutionary significance of
713 encephalization in some eutherian mammals: effects of adaptive radiation,
714 domestication, and feralization. *Brain, Behavior and Evolution*, **65**, 73-108.
715 doi: 10.1159/000082979.

716 Kruska, D.C.T. (2014) Comparative quantitative investigations on brains
717 of wild cavies (*Cavia aperea*) and guinea pigs (*Cavia aperea f. porcellus*).

A contribution to size changes of CNS structures due to domestication. *Mammalian Biology*, **79**, 230-239.

Larouche, M., Diep, C., Sillitoe, R.V. and Hawkes, R. (2003) Topographical anatomy of the cerebellum in the guinea pig, *Cavia porcellus*. *Brain Research*, **965**, 159-69. doi: 10.1016/s0006-8993(02)04160-4.

Larsen, J.O., Skalicky, M. and Viidik, A. (2000) Does long-term physical exercise counteract age-related Purkinje cell loss? A stereological study of rat cerebellum. *Journal of Comparative Neurology*, **428**, 213-222.

Larsen, J.O., Tandrup, T. and Braendgaard, H. (1993) Number and size distribution of cerebellar neurons estimated by the optical fractionator and the vertical rotator. *Acta Stereologica*, 12, 283-288.

Lee, K.H., Mathews, P.J., Reeves, A.M.B., Choe, K.Y., Jami, S.A., Serrano, R.E. and Otis, T.S. (2015) Circuit mechanisms underlying motor memory formation in the cerebellum. *Neuron*, **86**, 529-540.

Lev-Ram, V., Valsamis, M., Masliah, E., Levine, S. and Godfrey, H.P. (1993) A novel non-ataxic guinea pig strain with cerebrocortical and cerebellar abnormalities. *Brain Research*, **606**, 325-331.

Llinás, R. and Welsh, J.P. (1993) On the cerebellum and motor learning. *Current Opinion in Neurobiology*,**3**, 958-965.

Lossi, L., Marroni, P. and Merighi, P. (1997) Cell proliferation in the

739 cerebellar cortex of the rabbit and guinea pig. XXIst Congress of the
740 European Association of Veterinary Anatomists. *Anatomia Histologia*
741 *Embryologia*, **26**, 257.
742 Mallard, C., Loeliger, M., Copolov, D. and Rees, S. (2000) Reduced
743 number of neurons in the hippocampus and the cerebellum in the postnatal
744 guinea pig following intrauterine growth-restriction. *Neuroscience*, **100**,
745 327-333.
746 Mattfeldt, T., Mall, G., Gharehbaghi, H. and Möller P. (1990) Estimation
747 of surface area and length with the orientator. Journal of Microscopy, 159,
748 301-317.
749 Molinari, M., Chiricozzi, F.R., Clausi, S., Tedesco, A.M., De Lisa, M.
750 and Leggio, M.G. (2008) Cerebellum and detection of sequences: from
751 perception to cognition. *The Cerebellum*, **7**, 611-615.
752 Monjan, A.A., Gilden, D.H., Cole, G.A. and Nathanson, N. (1971)
753 Cerebellar hypoplasia in neonatal rats caused by lymphocytic
754 choriomeningitis virus. *Science*, **171**, 194-196.
755 Miyata, M., Miyata, H., Mikoshiba, K. and Ohama, E. (1999)
756 Development of Purkinje cells in humans: an immunohistochemical study
757 using a monoclonal antibody against the inositol 1,4,5-triphosphate type 1
758 receptor (IP3R1). *Acta Neuropathologica*, **98**, 226-32. doi:
759 10.1007/s004010051073.

760 Mwamengele, G.L., Mayhew, T.M. and Dantzer, V. (1993) Purkinje cell
761 complements in mammalian cerebella and the biases incurred by counting
762 nucleoli. *Journal of Anatomy*, **183**, 155-60.
763 Nishikimi, M., Kawai, T. and Yagi, K. (1992) Guinea pigs possess a
764 highly mutated gene for L-gulono-lactone oxidase, the key enzyme for L-
765 ascorbic acid biosynthesis, missing in this species. *Journal of Biological*
766 *Chemistry*, **267**, 21967-21972.
767 Noorafshan, A., Asadi-Golshan, R., Erfanizadeh, M. and Karbalay-
768 Doust, S. (2018) Beneficial effects of olive oil on the rats' cerebellum:
769 functional and structural evidence. *Folia Medica (Plovdiv)*, **60**, 454-463.
770 doi: 10.2478/folmed-2018-0022
771 Nyengaard, J.R. (1999) Stereologic methods and their application in
772 kidney research. *Journal of the American Society of Nephrology*, **10**, 1100-
773 1123.
774 Ragbetli, M.C., Ozyurt, B., Aslan, H., Odaci, E., Gokcimen, A., Sahin,
775 B. and Kaplan, S. (2007) Effect of prenatal exposure to diclofenac sodium
776 on Purkinje cell numbers in rat cerebellum: A stereological study. *Brain*
777 *Research*, **1174**, 130-135.
778 Raz, N., Dupuis, J.H., Briggs, S.D., McGavran, C. and Acker, J.D.
779 (1998) Differential effects of age and sex on the cerebellar hemispheres and
780 the vermis: a prospective MR study. *American Journal of Neuroradiology*,

19, 65-71.

Roostaei, T., Nazeri, A., Saharaian, M.A. and Minagar, A. (2014) The human cerebellum: a review of physiologic neuroanatomy. *Neurologic Clinics*, **32**, 859-869.

Sadeghinezhad, J., Aghabalazadeh Asl, M., Saeidi, A. and De Silva, M. (2020) Morphometrical study of the cat cerebellum using unbiased design-based stereology. *Anatomia Histologia Embryologia*, **49**, 788-797. doi: 10.1111/ahe.12583

Sato, N., Yagishita, A., Oba, H., Miki, Y., Nakata, Y., Yamashita, F. *et al*. (2007) Hemimegalencephaly: a study of abnormalities occurring outside the involved hemisphere. *American Journal of Neuroradiology*, **28**, 678-682.

Schmahmann, J.D. and Caplan, D. (2006) Cognition, emotion and the cerebellum. *Brain*, **129**, 290-292.

Schmitz C, Hof PR (2005) Design-based stereology in neuroscience. Neuroscience **130**:813-831.

Selçuk, M.L. and Tıpırdamaz, S. (2020) A morphological and stereological study on brain, cerebral hemispheres and cerebellum of New Zealand rabbits. *Anatomia Histologia Embryologia,* **49**, 90-96. doi: 10.1111/ahe.12489

Silva, F.M.O., Alcantara, D., Carvalho, R.C., Favaron, P.O., Santos,

A.C., Viana, D.C. and Miglino, M.A. (2016). Development of the central nervous system in guinea pig (*Cavia porcellus*, Rodentia, Caviidae). *Pesquisa Veterinária Brasileira*, **36**, 753-760 doi: 10.1590/S0100-736X2016000800013

Song, C.H., Bernhard, D., Hess, E.J. and Jinnah, H.A. (2014) Subtle microstructural changes of the cerebellum in a knock-in mouse model of DYT1 dystonia. *Neurobiology of Disease*, **62**, 372-380.

Sonmez, O.F., Odaci, E., Bas, O. and Kaplan, S. (2010) Purkinje cell number decreases in the adult female rat cerebellum following exposure to 900MHz electromagnetic field. *Brain Research*, **1356**, 95-101. doi: 10.1016/j.brainres.2010.07.103

Sørensen, F. W., Larsen, J. O., Eide, R. and Schiønning, J. D. (2000) Neuron loss in cerebellar cortex of rats exposed to mercury vapor: a stereological study. *Acta Neuropathologica*, **100**, 95-100. doi: 10.1007/s004010051198

Sterio, D.C. (1984) The unbiased estimation of number and sizes of arbitrary particles using the disector. *Journal of Microscopy*, **134**, 127-36.

Sultan, F. and Braitenberg, V. (1993) Shapes and sizes of different mammalian cerebella. A study in quantitative comparative neuroanatomy. *Journal fur Hirnforschung*, **34**, 79-92.

Taman, F.D., Kervancioglu, P., Kervancioglu, A.S. and Turhan, B. (2020)

The importance of volume and area fractions of cerebellar volume and vermian subregion areas: a stereological study on MR images. *Child's Nervous System*, **36**, 165-171. doi: 10.1007/s00381-019-04369-9.

Tunç, A.T., Turgut, M., Aslan, H., Sahin, B., Yurtseven, M.E. and Kaplan, S. (2006) Neonatal pinealectomy induces Purkinje cell loss in the cerebellum of the chick: a stereological study. *Brain Research*, **1067**, 95-102. doi: 10.1016/j.brainres.2005.10.011

Van Andel, R.A., Franklin, C.L., Besch-Williford, C., Riley, L.K., Hook, R.R. Jr. and Kazacos, K.R. (1995) Cerebrospinal larva migrans due to *Baylisascaris procyonis* in a guinea pig colony. *Laboratory Animal Science*, **45**, 27-30.

Vastagh, C., Víg, J., Takács, J. and Hámori, J. (2005) Quantitative analysis of the postnatal development of Purkinje neurons in the cerebellum of the cat. *International Journal of Developmental Neuroscience*, **23**, 27-35. doi: 10.1016/j.ijdevneu.2004.09.005.

Walhovd, K. B., Fjell, A. M., Reinvang, I., Lundervold, A., Dale, A. M., Eilertsen, D. E. *et al*. (2005) Effects of age on volumes of cortex, white matter and subcortical structures. *Neurobiology of Aging*, **26**, 1261-1270. doi: 10.1016/j.neurobiolaging.2005.05.020

Weber, U.J., Bock, T., Buschard, K. and Pakkenberg, B. (1997) Total number and size distribution of motor neuronsin the spinal cord of normal

844 and EMC-virus infected mice—a stereological study. *Journal of Anatomy*,
845 **191**, 347-353.
846 Welniak–Kaminska, M., Fiedorowicz, M., Orzel, J., Bogorodzki, P.,
847 Modlinska, K., Stryjek, R. *et al*. (2019) Volumes of brain structures in
848 captive wildtype and laboratory rats: 7T magnetic resonance in vivo
849 automatic atlas-based study. *PLoS One*, **14**, e0215348. doi:
850 10.1371/journal. pone.0215348
851 West, M.J. (1993) New stereological methods for counting neurons.
852 *Neurobiology of Aging*, **14**, 275-285.
853 Wittmann, W. and McLennan, I.S. (2011) The male bias in the number of
854 Purkinje cells and the size of the murine cerebellum may require Müllerian
855 Inhibiting Substance/Anti-Müllerian Hormone. *Journal of*
856 *Neuroendocrinology*, **23**, 831-838.
857 Woodruff-Pak, D.S. (2006) Stereological estimation of Purkinje neuron
858 number in C57BL/6 mice and its relation to associative learning.
859 *Neuroscience*, **141**, 233-243.
860 Woodruff-Pak, D.S., Foy, M.R., Akopian, G.G., Lee, K.H., Zach, J.,
861 Nguyen, K.P.T. *et al*. (2010) Differential effects and rates of normal aging
862 in cerebellum and hippocampus. *Proceedings of the National Academy of*
863 *Sciences*, **107**, 1624-1629.
864 Zhang, C., Hua, T., Zhu, Z. and Luo, X. (2006) Age-related changes of

structures in cerebellar cortex of cat. *Journal of Biosciences*, **31**, 55-60. doi: 10.1007/bf02705235

Table 1. Stereological data for total volume of cerebellar hemisphere and proportional volume of gray matter and white matter in six guinea pigs.

Animals	Cerebellum weight (g)	Total volume of cerebellum (weight/specific gravity) (cm^3)	Total volume of cerebellum (Cavalieri estimator) (cm^3)	Shrinkage (%)	Gray matter		White matter	
					Volume fraction (%)	Volume (cm^3)	Volume fraction (%)	Volume (cm^3)
1	0.257	0.247	0.117	54.47	75.94	0.1875	24.05	0.0594
2	0.282	0.271	0.118	58.15	80.42	0.2179	19.57	0.0530
3	0.298	0.286	0.117	60.73	77.60	0.2219	22.39	0.0640
4	0.263	0.252	0.079	69.96	78.64	0.1981	21.35	0.0538
5	0.280	0.269	0.112	60	74.37	0.2000	25.62	0.0689
6	0.335	0.322	0.118	64.77	81.42	0.2621	18.57	0.0597
Mean±SD	0.285±0.028	0.274±0.027	0.110±0.015	61.34±5.39	78.06±2.66	0.2145±0.0266	21.92±2.66	0.0598±0.0060

Table 2. Stereological data for surface area, volume and thickness of molecular and granular layers in cerebellar hemisphere in six guinea pigs.

Animals	1	2	3	4	5	6	Mean±SD
Surface area (mm^2)	486.066	555.984	630.003	627.302	592.925	776.140	611.40±96.8
Volume fraction of molecular layer (%)	40.28	42.24	39.3	41.63	34.42	46.19	40.67±3.87
Volume of molecular layer (mm^3)	99.4	114.4	112.3	104.9	92.5	151.0	112.41±20.56
Volume fraction of granular layer (%)	35.65	38.18	38.29	37.01	39.94	35.23	37.38±1.77
Volume of granular layer(mm^3)	88.0	103.4	109.5	93.2	107.4	113.4	104.38±7.31
Thickness of molecular layer(mm)	0.204	0.205	0.178	0.167	0.156	0.194	0.184±0.020
Thickness of granular layer(mm)	0.181	0.185	0.173	0.148	0.181	0.146	0.169±0.017

Table 3. Stereological data for numeral density and total number of Purkinje cells in cerebellar hemisphere in six guinea pigs.

Animals	1	2	3	4	5	6	Mean±SD
Numeral density (cells/mm^3)	2532	2413	2215	2546	2197	1986	2314.833 ± 220.099
Total number	296010	284380	258570	200660	245280	233640	253090 ± 34754

Table 4. The mean coefficient of error (CE) and coefficient of variation (CV) of stereological analysis of guinea pig cerebellum (n=6)

	Total volume	Grey matter volume	White matter volume	Granular layer volume	Molecular layer volume	Surface area	Total number of Purkinje cells
CE	0.016	0.080	0.050	0.033	0.031	0.0162	0.080
CV	0.140	0.123	0.101	0.096	0.182	0.158	0.137
CE^2/CV^2	0.013	0.423	0.252	0.121	0. 029	0.479	0.346

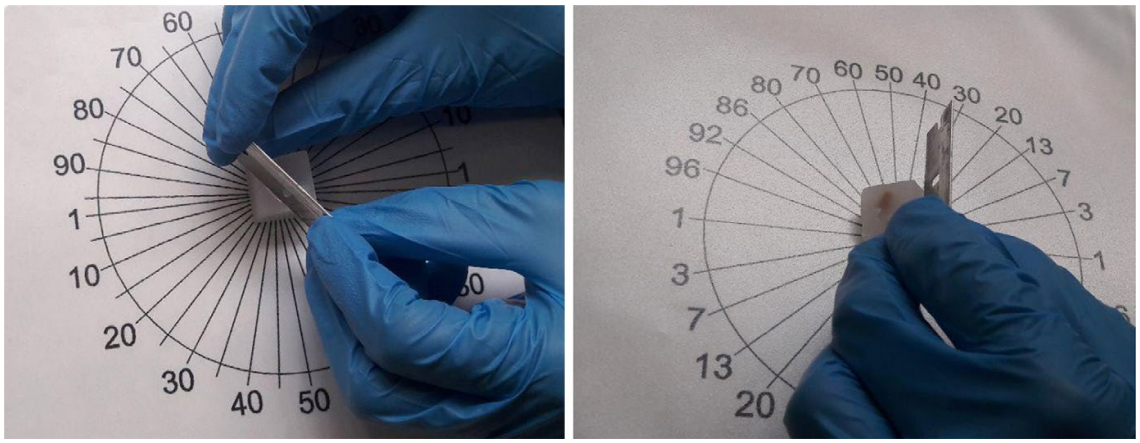

Figure 1. Isotropic, uniform random sections of the guinea-pig cerebellar hemispheres were obtained by applying the orientator method. (a): A randomly chosen cerebellar hemisphere for each animal was embedded in a paraffin block and placed at the centre of a circle with 90 equidistant divisions along the perimeter. A random number between 0 and 90 was looked up and the paraffin medium was cut along a line parallel to the direction of the selected number (here, 75). (b): The block was placed on its cut surface at the center of a second circle, with 96 nonequidistant divisions along its perimeter. The paraffin was cut along a line parallel to the direction of a random number ranging from 0 to 96 (here, 50), and the block was finally re-embedded in paraffin while placed on its cut surface, and consecutive 25 µm-thick sections were cut with a microtome.

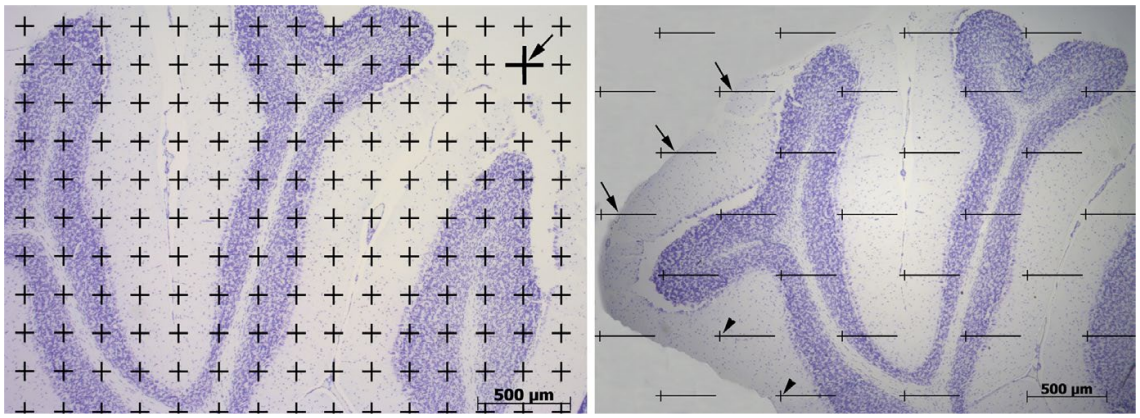

Figure 2. Estimation of cerebellar volume and surface area by employing the point-counting and the test-lines systems. (a): The volume of the cerebellar structures was estimated by randomly superimposing a point-counting probe onto each section. The upper right corner of each point (arrow) was taken as a reference for the count of the number of points hitting the region of interest. (b): The surface area of the cerebellum was estimated by superimposing test-lines onto each section. The arrowheads show two points hitting the molecular layer, whereas the arrows indicate the intersection between test lines with the outer cerebellar surface.

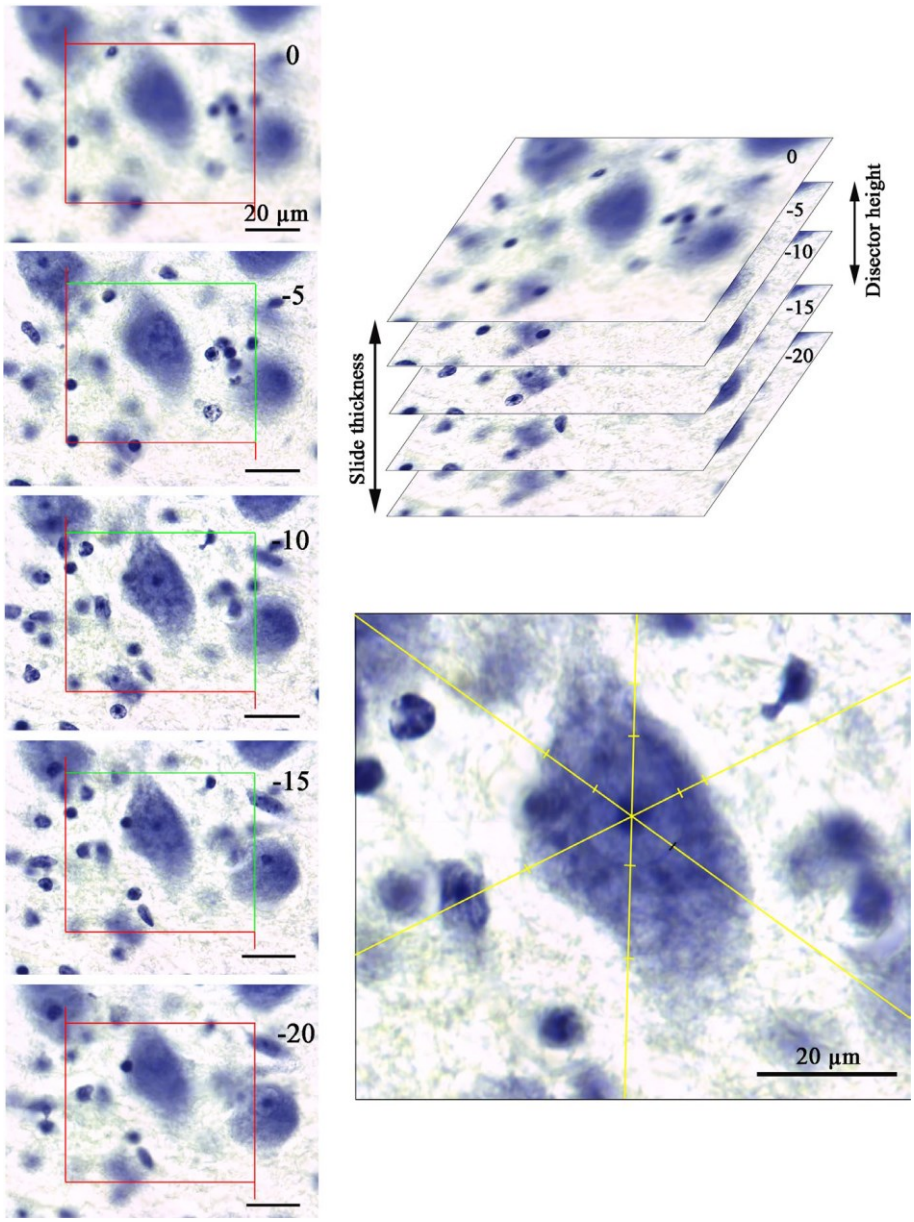

Figure 3. Use of the optical disector technique for the Purkinje cell count and of the nucleator technique for the estimation of the Purkinje cellular and nuclear volumes. **(a):** The microscopic fields were selected by moving the microscope stage in the x and y directions for a constant distance. Then, the stage of microscope moved in z-axis and the consecutive focal planes were evaluated within optical disector height (10 µm from -5 to -15 µm).

(b-f): The unbiased counting frame principle was applied for the Purkinje ell count. The cells whose nucleolus was located inside the counting frame or crossed the accepted lines were sampled, and those whose nucleolus came into focus within disector height were counted. (g): The intercept length from the nucleolus to the border of the cytoplasm, or to the border of the nucleus, was measured for the estimation of Purkinje cellular and nuclear volumes, respectively.

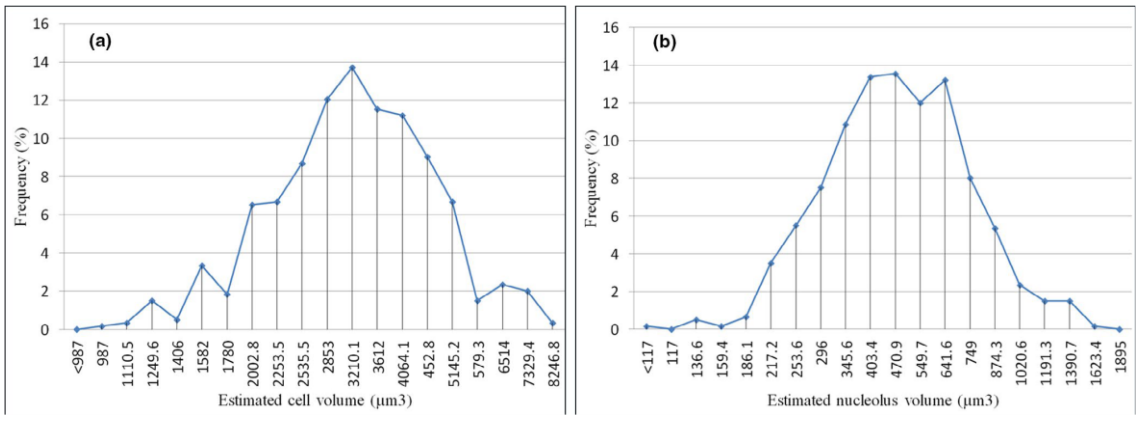

Figure 4. Graphs showing the frequency distribution of the Purkinje cellular (a) and nuclear (b) volumes in the guinea-pig cerebellum.